BJA

British Journal of Anaesthesia, xxx (xxx): xxx (xxxx)

doi: 10.1016/j.bja.2020.11.035
Advance Access Publication Date: xxx
Laboratory Investigation

LABORATORY INVESTIGATION

Propofol sedation-induced alterations in brain connectivity reflect parvalbumin interneurone distribution in human cerebral cortex

Michael M. Craig[1,2,*], Bratislav Misic[3], Ioannis Pappas[1,2], Ram M. Adapa[1,2], David K. Menon[1,2] and Emmanuel A. Stamatakis[1,2]

[1]Division of Anaesthesia, Department of Medicine, School of Clinical Medicine, University of Cambridge, Cambridge, UK, [2]Wolfson Brain Imaging Centre, Department of Clinical Neurosciences, School of Clinical Medicine, University of Cambridge, Cambridge, UK and [3]Montreal Neurological Institute, McGill University, Montreal, QC, Canada

*Corresponding author. E-mail: mmc57@cam.ac.uk

Abstract

Background: Propofol, a commonly used intravenous anaesthetic, binds to type A gamma aminobutyric acid (GABA) receptors in mammalian brain. Previous work on its anaesthetic action has characterised either the biochemistry underlying propofol binding or the associated changes in brain network dynamics during sedation. Despite these advances, no study has focused on understanding how propofol action at the cellular level results in changes in brain network connectivity.

Methods: We used human whole-brain microarray data to generate distribution maps for genes that mark the primary GABAergic cortical interneurone subtypes (somatostatin, parvalbumin [PV], and 5-hydroxytryptamine 3A. Next, 25 healthy participants underwent propofol-induced sedation during resting state functional MRI scanning. We used partial least squares analysis to identify the brain regions in which connectivity patterns were most impacted by propofol sedation. We then correlated these multimodal cortical patterns to determine if a specific interneurone subtype was disproportionately expressed in brain regions in which connectivity patterns were altered during sedation.

Results: Brain networks that were significantly altered by propofol sedation had a high density of PV-expressing GABAergic interneurones. Brain networks that anticorrelated during normal wakefulness, namely the default mode network and attentional and frontoparietal control networks, increased in correlation during sedation.

Conclusions: PV-expressing interneurones are highly expressed in brain regions with altered connectivity profiles during propofol-induced sedation. This study also demonstrates the utility of leveraging multiple datasets to address multiscale neurobiological problems.

Keywords: default mode network; frontoparietal control network; functional connectivity; GABAergic interneurone; gene expression; parvalbumin; propofol

Editor's key points

- It is not clear how propofol action at the cellular level results in changes in brain network connectivity to produce sedation.
- Whole-brain microarray data were used to identify the primary GABAergic cortical interneurone subtypes for correlation with propofol-induced changes in resting state functional MRI scanning.
- Brain networks that were significantly altered by propofol sedation had a high density of parvalbumin-expressing GABAergic interneurones.
- Parvalbumin-expressing interneurones are highly expressed in brain regions with altered connectivity induced by propofol sedation.

General anaesthesia is a reversible drug-induced state of unconsciousness that is maintained for the duration of surgical

Received: 14 October 2019; **Accepted:** 10 November 2020

© 2020 The Authors. Published by Elsevier Ltd on behalf of British Journal of Anaesthesia. This is an open access article under the CC BY license (http://creativecommons.org/licenses/by/4.0/).
For Permissions, please email: permissions@elsevier.com

and non-surgical medical procedures. One of the most frequently used general anaesthetics is propofol, a gamma aminobutyric acid (GABA)ergic drug that increases inhibitory tone in neurones throughout the CNS.[1–3] Despite an understanding of its primary receptor target,[4] little is known about how these molecular and cellular processes influence the macro-scale cortical network mechanisms that result in propofol-induced anaesthesia and sedation.

Functional connectivity of the functional MRI (fMRI) blood-oxygenation-level-dependent (BOLD) signal is commonly used to study brain network connectivity.[5] Functional connectivity during propofol sedation has been shown to decrease within networks typically thought to be important for high-level cognition, including the default mode network (DMN) and the executive control network (ECN).[6,7] These networks are typically thought to be anticorrelated during resting wakefulness.[8] However, several studies have shown that as sedation increases, the anticorrelation between these networks decreases.[6,9] This body of work suggests that propofol induces loss of consciousness, at least partially, by disrupting synchronous and asynchronous patterns within large-scale brain networks.

We used multivariate statistical methods with human functional imaging data to identify whether patterns of cortical network dynamics are reflected in the distribution of one or more GABAergic interneurone subtypes. We first generated cortical expression maps for parvalbumin (PV), somatostatin (SST) and 5-hydroxytryptamine 3a (5-HT3A) receptors[10] using the Allen Institute for Brain Science (AIBS) Human Microarray dataset.[11] Next, we used fMRI data from 25 healthy participants undergoing propofol sedation to identify patterns of connections that were collectively affected by propofol sedation. We then correlated these measures to find associations between different GABAergic interneurones and the pattern of functional connectivity resulting from sedation.

Methods

Gene expression maps

The AIBS Human Brain Atlas (HBA) is a publicly available resource of microarray gene expression profiles across a set of brain regions.[11] A DNA microarray consists of a number of DNA probes attached to a fixed surface. It allows for the concentration of a large number of transcribed mRNAs in a sample tissue to be quantified. The atlas uses *postmortem* tissue from six donors, none of whom had a history of neurological or neuropsychiatric disease and who passed a strict set of serology, toxicology, and RNA quality screens. The following steps were taken by the AIBS to generate and validate the HBA data. After each step, a minimum specified quantity of tissue was saved for the following processing step. Tissue collection and initial processing occurred at independent tissue banks. Tissue was frozen and shipped to the Allen Institute for further processing. After screening and quality control, large format histology data were taken from each slab with 4.65 μm/pixel digital image resolution. This tissue slab was divided into smaller blocks organised based on whether they contained cortical or subcortical structures. These blocks were then sectioned for histology data with a final image resolution of 1 μm/pixel. Subcortical blocks were further sectioned onto membrane slides that allow laser microdissection of these structures. Anatomically defined samples were used for microarray analysis by manual macrodissection of the remaining tissue from each block (for cortical and some subcortical structures) or by laser-based microdissection (subcortical and brainstem regions). RNA samples that passed quality control were sent for microarray analysis at Beckman Coulter Genomics. Data were then returned to the Allen Institute and subjected to further quality control, normalisation, and analysis before inclusion in the final dataset.

The normalisation procedure consisted of both within-brain and between-brain steps. The within-brain steps included preprocessing of array-specific biases and 75th percentile alignment of distributions of all samples within a batch. Adjustments were then made for RNA quality differences among samples within a batch. Batch-to-batch variance was adjusted using internal (pooled RNA comprising 150–300 cortical samples) and HBA (pooled RNA from 300 cortical macro samples from the first HBA brain) control datasets. Adjustments were then made for differences in dissection methods. For between-brain normalisation, brain-wise mean expression levels were aligned, resulting in normalised z-scores for each gene intensity distribution in each brain region. For more details on the AIBS HBA, please see the AIBS technical white papers (https://help.brain-map.org/display/humanbrain/Documentation).

We overlapped the centres of each region in our MRI parcellated data to the Montreal Neurological Institute (MNI) coordinates of the samples from the AIBS dataset.[12,13] If multiple probes were present in one region of interest (ROI), we averaged the gene expression. We used a published gene list to discard probes that did not match gene symbols presented in the AIBS dataset.[14] This generated a matrix with 20 737 rows (corresponding to different genes) and 118 columns (corresponding to different regions). The cells in this matrix indicate the expression of a particular gene in each brain region. To create gene expression maps for PV, SST, and 5-HT3a we indexed this matrix taking all probes that corresponded to each gene. This gave us a column vector that represented expression for each gene in each brain region. As previous work has shown that gene expression is largely bilaterally symmetric, especially in primary visual regions,[15] we validated our maps by testing for significant differences between hemispheres of the visual network. To do so, we performed a t-test between gene expression in eight visual regions from the left hemisphere and eight visual regions from the right hemisphere. We used the unthresholded bootstrap ratio (BSR) matrix and summed the values across each row, resulting in a column vector representing the contribution weight for each region. We then used a Pearson's correlation to assess whether there was a statistical relationship between a region's change in connectivity during propofol sedation and its expression of PV, SST, or 5-HT3a. All correlations with gene expression maps were significant using either the thresholded or unthresholded BSR matrices.

Sedation procedure

Approval for this study was obtained from the Cambridgeshire 2 Regional Ethics committee. We recruited 25 healthy participants (nine female; mean age 35 [range 19–53] yr). Two senior anaesthetists were present during the entire session to observe participants. Propofol administration was delivered i.v. as a target-controlled infusion (plasma concentration mode) using an Alaris PK infusion pump (Carefusion,

Basingstoke, UK) programmed with the Marsh pharmacokinetic model.[16,17] There were four conditions, with three different plasma target levels: (1) no drug 1 (baseline), (2) 0.6 μg ml^{-1} (low sedation), (3) 1.2 μg ml^{-1} (moderate sedation), and (4) no drug 2 (recovery). There was a 10 min period that allowed for equilibrium between plasma and effect-site propofol concentration before cognitive tests began. Blood samples were drawn (a total of six) at the end of each titration period and before the plasma target was altered.

Sedation level was assessed verbally before and after each scanning run. At low sedation levels, all participants displayed slow response to their name spoken in a normal tone (based on Observer's Assessment of Alertness/Sedation Scale [OAA/S] scores of 4, or a Ramsay score of 2). At moderate levels of sedation, all participants were more deeply sedated and responded only when their name was spoken loudly (corresponding to an OAA/S score of 3, or a Ramsay score of 3). TIVATrainer (pharmacokinetic simulation software package; www.eurosiva.org) showed that plasma concentrations would asymptotically approach zero 15 min after propofol sedation. Therefore, recovery scans were acquired at 20 min after cessation of propofol. Mean plasma propofol concentration was 305 (standard deviation [SD]=14) ng ml^{-1} during light sedation, 723 (SD=320) ng ml^{-1} during moderate sedation, and 276 (SD=75) ng ml^{-1} during recovery. The mean total mass of propofol administered was 210 (SD=33) mg, equal to 3.0 (SD=0.47) mg kg^{-1}.

Data acquisition

A Trio Tim 3T MRI system (Siemens, Erlangen, Germany) was used to collect structural data. A 12-channel head matrix transmit-receive coil, using a fast-sparse 32 slice axial oblique sequence was used (repetition time (TR)=2s, echo time (TE)=30 ms, flip angle=78, voxel size=3.0×3.0×3.0 mm, matrix size 64×64, field of view 192 mm×192 mm, slice thickness=3.0 mm, 0.8 mm gap between slice, bandwidth=2422 Hz per Px). A total of 150 echo planar images (EPI) were collected per sedation condition (600 across the entire scanning session). T1-weighted MPRAGE high-resolution structural images were also acquired at 1 mm isotropic resolution (TR=2250 ms, TI=900 ms, TE=2.99 ms, flip angle=9).

MRI data preprocessing

Image preprocessing was performed using Statistical Parametric Mapping (SPM) 12 (http://www.fil.ion.ucl.ac.uk/spm/). The first five images for each sedation level were removed to eliminate saturation effects and achieve steady-state magnetisation. All functional data were slice-time corrected and motion-corrected. Structural images were co-registered to the mean EPI and segmented into grey matter, white matter, and CSF masks, then normalised to the MNI space with a resolution of 2×2×2 mm.[18] Functional images were then smoothed with a 6 mm FWHM Gaussian kernel. To mitigate movement-related and physiological noise, data underwent despiking with a hyperbolic tangent squashing function, followed by the aCompcor technique. This process removes the first five principal components of the signal from white matter and CSF masks, and six motion parameters and their first-order temporal derivatives and a linear detrending term. Images were then high pass filtered to remove low-frequency fluctuations attributable to scanner noise (0.009 Hz<f).[19]

Creating functional connectivity matrices

The Conn functional connectivity toolbox was used to extract time series from a set of predefined ROI.[20] The Lausanne parcellation, a commonly used brain region parcellation template,[21] was used to define a set of 129 cortical brain regions. Because the present study was focused exclusively on large-scale cortical brain networks, 11 subcortical brain regions were removed from the analysis, leaving a total of 118 regions. ROI time courses were created by extracting the signal in each volume for each brain region for all four sedation conditions across subjects. Regional time series across each individual sedation level were then correlated, creating individual subject connectivity matrices for each sedation condition.

Partial least squares analysis

Partial least squares (PLS) is a multivariate statistical analysis used to identify relationships between sets of variables[22,23] that aims to identify linear combinations of variables in each set that maximally covary with each other. In the current analysis, this corresponds to a weighted combination of functional connections that maximally explain a pattern associated with changing levels of sedation. Singular value decomposition (SVD) functional data for each sedation condition were organised in a matrix containing each unique connection (corresponding to the upper elements of the connectivity matrix) for each subject stacked on top of each other. With n=118 nodes, this corresponds to k=118×(118−1)/2=6903 unique connections per condition. Thus, the data matrix contains k=6903 columns and N=100 rows (that is, 25 subjects×four conditions). We used a mean-centred approach where connection strengths are expressed as a deviation from the grand mean across the entire data set. This matrix, X, then underwent SVD:

$$\mathbf{X}=\mathbf{U}\Delta\mathbf{V}'$$

Such that

$$\mathbf{U}'\mathbf{U}=\mathbf{V}'\mathbf{V}=\mathbf{I}$$

This analysis yields a set of orthogonal latent variables (LVs), where U and V are matrices of left and right singular vectors and Δ is a matrix with singular values along the diagonal and zeros elsewhere. Singular vector elements weigh the contribution of individual variables (connections across sedation condition) to the overall multivariate pattern. The proportion of covariance between functional connectivity and study design captured by an LV serves as a measure of effect size, and is estimated as the ratio of the squared singular value to the sum of squared singular values from the SVD.[24]

Assessing significance of LVs with permutation tests

Each LV was tested for statistical significance using permutation tests by randomly reordering the rows (i.e. condition labels: baseline, low sedation, moderate sedation, and recovery) of the original X matrix. The permuted matrices were then mean-centred and subjected to SVD as described above. This process creates a distribution of singular values under the null hypothesis so that there is no relationship between study design (sedation conditions) and functional connectivity. As singular values are proportional to the effect size of the LV, a P-

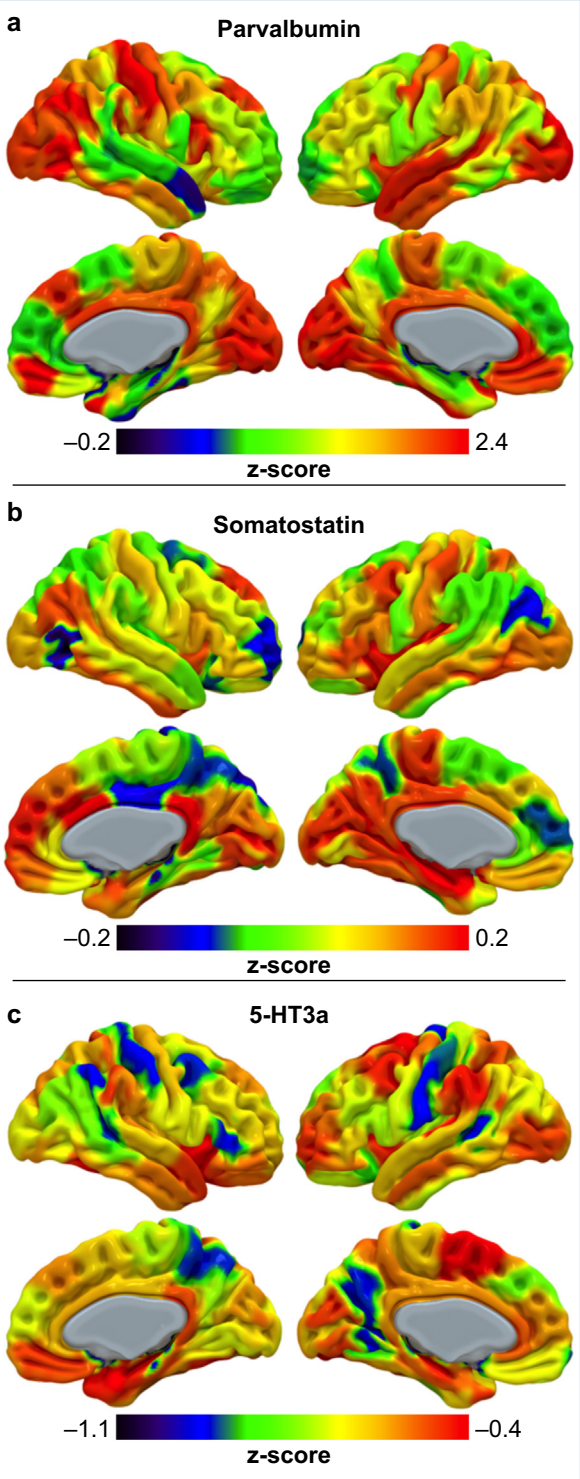

Fig 1. Cortical expression maps of gamma aminobutyric acid (GABA)ergic interneurons. Each map was created using the Allen Institute for Brain Science (AIBS) Human Microarray database. This database has microarray expression values for 20 737 genes across six subjects. The maps show an average value in each region across each of the six subjects. (a) Cortical expression of parvalbumin. (b) Cortical expression of somatostatin. (c) Cortical expression of 5-hydroxytryptamine 3a (5-HT3A).

value for each LV was estimated as the number of times the permuted singular values exceeded the original singular value.

Assessing the contribution and reliability of specific connections

We used bootstrap resampling to assess the contribution and reliability of each connection to the overall multivariate pattern. This process allows the patterns derived for each LV to be cross-validated. The algorithm creates new data matrices that resamples participants with replacement and performs SVD generating a sampling distribution for each weight in the singular vector. This bootstrap distribution can then be used to estimate the standard error of each connection weight. We then calculated a 'bootstrap ratio' for each connection by dividing the weight from the singular vector by its bootstrap-estimated standard error. A BSR with a large magnitude (positive or negative) signifies that the connection makes a large contribution to the LV and is stable across participants.

Brain network analysis

The output of our PLS analysis consisted of a single 118×118 matrix that contained a BSR for each connection. BSR are equivalent to z-scores if their distribution is approximately normal.[25] Thus, connections were thresholded at the 95% confidence interval (corresponding to z=1.96). Each ROI in our parcellation was overlapped with previously defined large-scale functional connectivity networks.[26] In order to focus our analysis on large-scale and bilateral networks, we modified a subset of these networks by collapsing all visual networks into one and also combining the left and right frontoparietal network into one network. This resulted in six large-scale networks, that included the auditory network (Aud), DMN, frontoparietal control network (FPCN), salience network (SN), somatomotor network (SM), and visual network (Vis). To assess the contribution of each network to the significant LV (i.e. the pattern of connectivity associated with changes in propofol sedation), we averaged the BSR within and between each large-scale network, including any connections with a value of 0. This allowed us to control for the fact that some networks have more ROIs and therefore more possible connections than others.

Results

Distribution of GABAergic interneurone gene expression in the human cortex (Fig. 1) shows the concentration of each of the three genes of interest across the cortex. PV (Fig. 1a) had a higher expression in comparison to either SST or 5-HTR3A. Highest expression was observed in the Vis, SM, and midline areas associated with the DMN. SSTR (Fig. 1b) was less expressed than PV across the cortex, with high expression in higher cognitive networks including the FPCN, SN, and DMN. Interestingly, SSTR showed a somewhat asymmetrical expression between the hemispheres, with qualitatively greater expression in the left hemisphere compared with the right hemisphere. HTR3A (Fig. 1c) was the least expressed of the three genes and was expressed mostly in Aud, DMN, and SN. To validate the expression maps we examined whether there were interhemispheric differences in expression of each of the GABAergic interneurone subtypes (Fig. 2). Specifically, we used *t*-tests to compare expression measures from the left and right hemispheres of the visual network (eight regions per

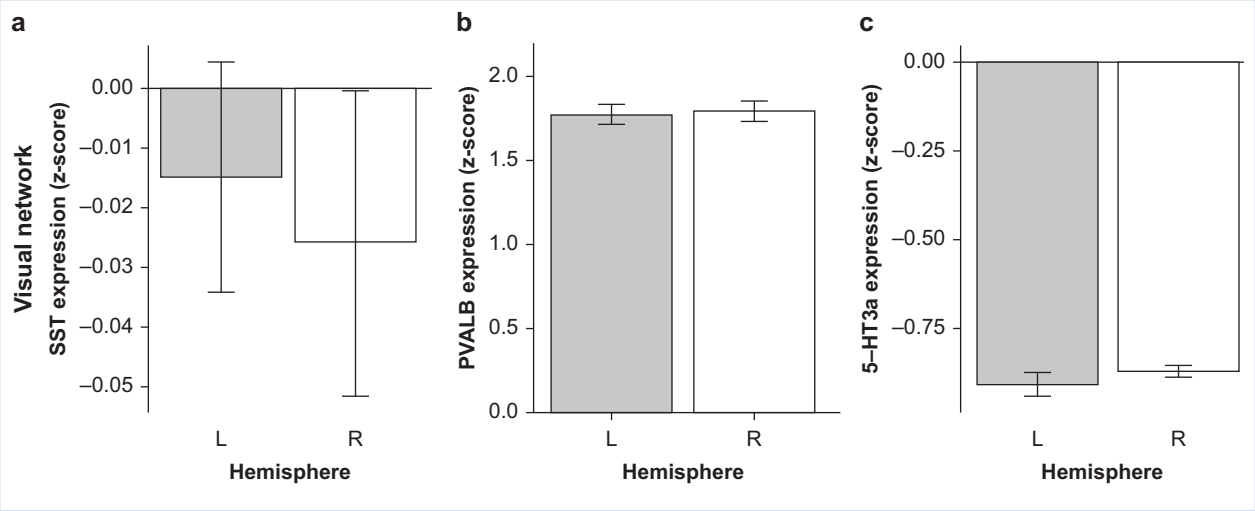

Fig 2. Testing for significant differences in gamma-aminobutyric acid (GABA)ergic interneuron gene expression between hemispheres. (a–c) There are no significant differences in expression of somatostatin (SST), parvalbumin (PVALB) or 5-hydroxytryptamine 3a (5-HT3A) between left (L) and right (R) hemispheres in the visual network. These measurements represent averages across each of the six subjects from the Allen Institute for Brain Science (AIBS) dataset.

hemisphere). We found no differences in the left, right comparisons of expression of PV (P=0.35), SST (P=0.83) or 5-HT3A (P=0.07).

Cortical functional connectivity patterns during propofol sedation

The output of the PLS analysis was a set of four LVs, each with a corresponding set of weights for each connection. Each LV represents a weighted pattern of functional connectivity that optimally covaries with the changing level of sedation. To determine statistical significance, each LV was subjected to permutation testing. This process identified only one of the four LVs and its associated weights to be significant (covariance accounted for was 22.3%, P=0.000009), therefore this LV was selected for further analysis. The resulting set of connections from this LV (Fig. 3a) followed one of two inverse patterns of connectivity (Fig. 3b). Each connection in the matrix corresponds to a BSR, that is, the weight of a connection divided by its bootstrap estimated standard error. The distribution of the BSR were not inconsistent with being from a normal distribution based on results from the D'Agostino and Pearson's test that combines skew and kurtosis to produce an omnibus test for normality (statistic=2.66, P-value=0.264). Connections with positive BSR scores follow a pattern of connectivity where, during the awake condition, connections displayed low levels of connectivity, but as propofol concentrations increased, these connections increased connectivity, then during recovery from sedation, levels of connectivity decreased to near awake levels. Brain regions that closely followed this pattern can be seen in Figure 3c. In contrast, connections with negative BSR scores were highly connected during the awake condition, then, as propofol concentrations increased, they decreased connectivity. During recovery, these connections then regained the level of connectivity they had during the awake condition. Brain regions that had connections which followed this pattern can be observed in Figure 3d. This finding confirms that patterns of functional connections follow one of two inverse trajectories during propofol administration, with some connections increasing as a function of sedation while others decrease.

We next examined connectivity patterns within six canonical large-scale brain networks. The positive BSR matrix (Fig. 4a) shows that DMN (Fig. 4b) and FPCN both contain connections that increase in connectivity strength during sedation. These networks also showed a significant number of between network connections that increase in strength as propofol sedation increases (Fig. 4c). Connections between DMN and Aud and SN also increased connectivity during propofol sedation. For the negative BSR matrix (Fig. 4d) a subset of within-DMN (Fig. 4e) and Vis-SM internetwork (Fig. 4f) connections decreased connectivity during propofol sedation.

Propofol-induced loss of connectivity is reflected by cortical parvalbumin expression

Our final aim was to determine whether these changing patterns of functional connectivity are reflected by the distributions of specific GABAergic interneurone subtypes. A significant correlation would suggest that there is a relationship between the connectivity profile and the presence of a GABAergic interneurone subpopulation. No significant relationship was found between SSTR expression and positive (r=0.093, P=0.31; Fig. 5a) or negative (r=−0.135, P=0.14; Fig. 5d) connectivity profiles. We found a significant positive correlation between PV expression and negative BSR connectivity profile (r=0.273, P=0.0028, Bonferroni corrected P=0.0168; Fig. 5e) but not for positive profile (r=−0.136, P=0.14; Fig. 5b). There was no significant relationship between 5-HT3A expression and positive connectivity profile (r=0.189, P=0.05; Fig. 5c), however, there was a negative trend (not significant when corrected for multiple comparisons) for HT3A expression and the negative connectivity profile (r=−0.199, P=0.0305, Bonferroni corrected P=0.183; Fig. 5f).

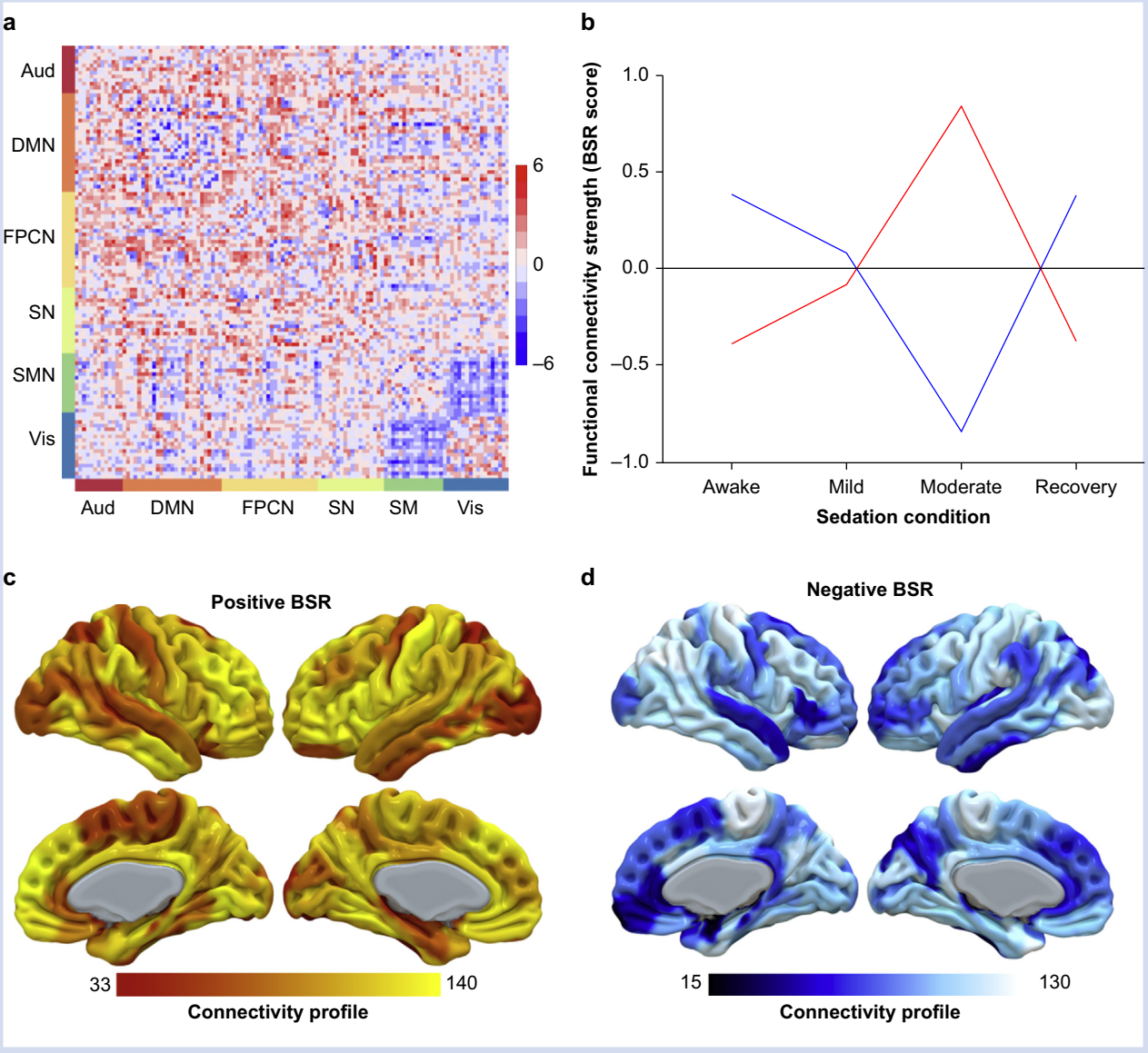

Fig 3. Inverse patterns of functional connectivity during propofol sedation. (a) BSR scores for each connection between regions. These are organised into six large scale cortical functional networks (auditory network [Aud], default mode network [DMN], frontoparietal control network [FPCN], salience network [SN], somatomotor network [SMN], and visual network [Vis]). (b) Patterns of connectivity that correspond to connections with positive BSR scores (red), negative BSR scores (blue). (c,d) Regional connectivity maps created by summing the BSR scores for each connection, resulting in an overall connectivity weight for each region. Higher values correspond to that region having a high number and highly weighted BSR scores that either gain or lose connectivity during sedation. (c) Regions that gain connections during sedation. (d) Regions that lose connections during sedation. BSR, bootstrap ratio.

Discussion

The aim of the present study was to determine whether a specific GABAergic interneurone subtype is important in mediating alterations in cortical brain network connectivity seen in propofol sedation. We hypothesised that PV-positive interneurones would be particularly important in driving this process, as they are important in longer range connectivity in animal models.[27–30] To assess this question, we first characterised the cortical expression pattern of three GABAergic interneurone subtypes (PV, SST, and 5-HT3a) using the AIBS Microarray database. Next, using fMRI data and the multivariate statistical technique PLS, we found a pattern of connectivity that corresponded to connections that either increased or decreased in connectivity strength during sedation, and returned to their initial levels during recovery. The regions that disproportionately reduced their connectivity during sedation significantly overlapped with the pattern of PV expression in the cortex. Taken together, our findings suggest that PV expression is higher in regions that reduce their cortical connectivity strength during propofol-induced sedation.

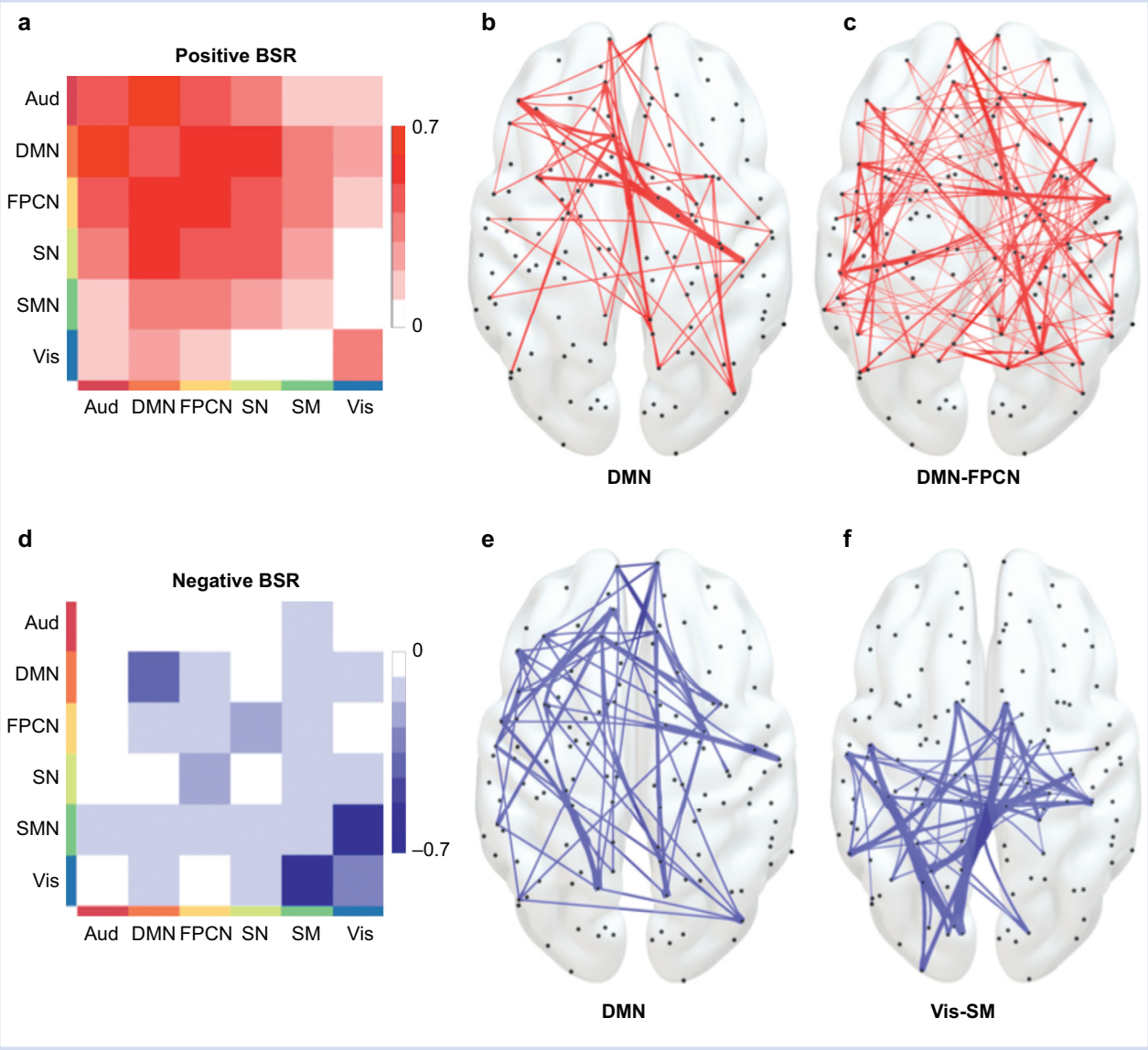

Fig 4. Network level alterations in functional connectivity during propofol sedation. (a) Positive BSRs collapsed across large scale networks and represents the degree to which individual networks increase within or between network connectivity during propofol sedation. (b) Within-DMN and (c) DMN-FPCN internetwork connections that increase their connectivity during sedation. (d) Negative BSRs collapsed across large scale networks and represents the degree to which each network decreases within and between network connectivity during sedation. (e) Within-DMN and (f) Vis-SM internetwork connections during propofol sedation. Aud, auditory network; BSR, bootstrap ratio; DMN, default mode network; FPCN, frontoparietal control network; SMN, somatomotor network; SN, salience network; Vis, visual network.

Parvalbumin expression is high in regions with attenuated connectivity during propofol sedation

We sought to determine whether different GABAergic interneurone subtypes are disproportionately expressed in regions greatly affected by propofol-induced sedation. This was motivated by previous work showing that propofol binds with high affinity to the β subunit of the $GABA_A$ receptor.[4] Using the AIBS Human Microarray database we constructed expression maps for PV, SST, and the 5-HT3a receptor that mark three subtypes of GABAergic interneurones found in the cortex.[10,31]

We found that regions that lost connectivity correlated significantly with regions with high PV expression. Although we cannot examine it directly because of the low sampling frequency of fMRI, this finding is potentially reflective of the loss of long distance gamma coherence during sedation.[32,33] Gamma oscillations are thought to be essential for binding neuronal assemblies and playing an important role in various cognitive processes including memory, sensation, and emotion.[34–36] Interconnected PV interneurones induce gamma oscillations through multiple means.[29,37,38] However, because fMRI is only a proxy for regional neuronal activity and

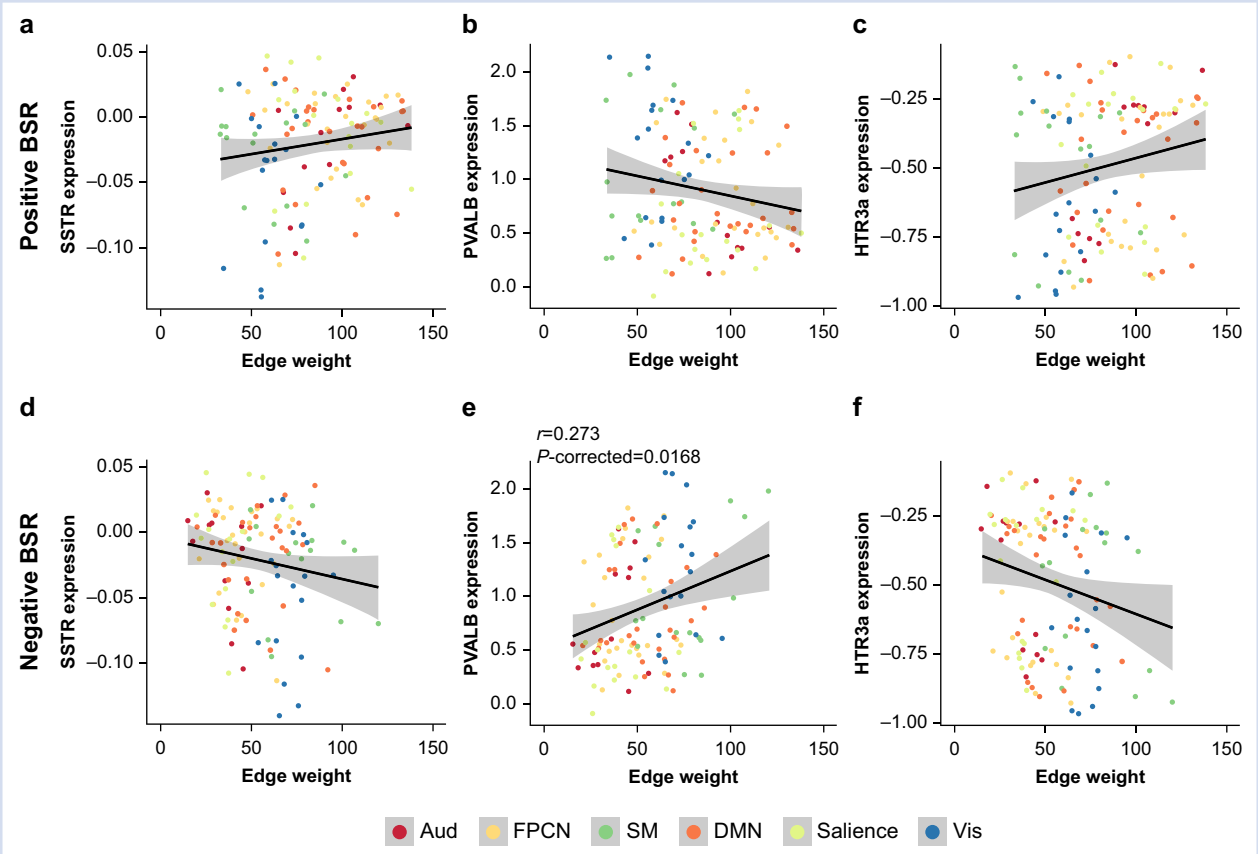

Fig 5. Correlating regional connectivity values with cortical interneuron gene expression. These graphs show correlations with the regional connectivity values shown in Figure 4 with the cortical distribution of interneuron gene expression shown in Figure 3. The top row shows correlations with regions that increase connectivity during sedation and the bottom row shows correlations with regions that decrease connectivity during sedation. The first column (a, d) shows correlations with somatostatin, the middle column (b, e) shows correlations with parvalbumin, and the third column (f, c) shows correlations with 5-HT3a. (e) Significant positive correlation between regions that lose connectivity during sedation and parvalbumin expression (r=0.273, P=0.0028, Bonferroni corrected P=0.0168). (f) Marginally significant (does not survive correction or multiple comparisons) negative correlation between regions that lose connectivity and expression of 5-HT3a (r=−0.199, P=0.0305, Bonferroni corrected P=0.183). Aud, auditory network; BSR, bootstrap ratio; DMN, default mode network; FPCN, frontoparietal control network; 5-HTR3A, 5-hydroxytryptamine 3a; PVALB, parvalbumin; SMN, somatomotor network; SST, somatostatin; Vis, visual network.

because of its low sampling frequency, it is beyond the scope of this study to connect macro-scale patterns of cortical connectivity with physiological processes such as local gamma oscillations. However, future work using electrophysiological methods could address the connection between PV interneurones, gamma oscillations, and sedation.

Brain network connectivity during propofol sedation

Cortical networks follow one of two dynamic patterns of connectivity, both of which are likely to disrupt information processing and ultimately lead to loss of consciousness. Previous work has found that anaesthetic drugs cause sedation and unconsciousness by altering cortical integration.[32] The present results are consistent with this hypothesis by finding that loss of integration is not simply the loss of connectivity between regions, but also increased connectivity between regions and networks that are typically anticorrelated in the awake, healthy human brain,[8] as has been observed previously. One study used seed-to-voxel functional connectivity to measure changes in posterior cingulate cortex (PCC) connectivity, a primary node in the DMN, during propofol sedation.[9] The PCC increased connectivity with regions of the ECN, including the anterior cingulate cortex at deeper levels of sedation, and with precentral gyrus and pontine tegmentum. This effect has also been observed in monkeys undergoing anaesthesia.[39]

Increases in connectivity between networks that are normally anticorrelated has also been observed in patients with disorders of consciousness. A recent study examined functional connectivity in patients with unresponsive wakefulness syndrome, minimally conscious state, emergence from minimally conscious state, and control subjects; subjects with more severe pathology had significantly reduced within DMN connectivity and greater between network connectivity with DMN and putative task positive regions (referred to as 'negative default mode network connectivity').[40] They also found

that brain metabolism, as measured by fluorodeoxyglucose-positron emission tomography scanning, was significantly correlated with positive and negative DMN connectivity. Patients who emerged from the minimally conscious state retained between-network anticorrelations, suggesting this measure could be used as a biomarker for prognosis. Our results reinforce these findings, suggesting that between DMN-task positive network connectivity generally reflects level of consciousness and is not specific to a particular drug or pathology. However, recent work has shown that a single common pathway between network connectivity may not reliably correlate with anaesthetic state. In two separate studies, one in surgical patients[41] and another in healthy subjects,[42] EEG data showed that during anaesthesia, brain networks display a dynamic interplay between different states. This is in contrast to previous approaches that aimed to identify a static state of equilibrium that reflects the anesthetised state.

We show that brain networks that contain connections with a negative BSR are enriched in PV expression. The DMN contains a number of highly weighted positive and negative BSR connections, however, only the regions with many negative connections correlate with PV expression. There is increasing evidence that the DMN contains multiple sub-networks that play different roles in cognitive and behavioural tasks.[43] Future work could directly investigate whether different sub-networks within DMN and within other large-scale brain networks differentially express PV.

Limitations

There are several limitations to this study that should be explored in future work. Most notably is that the fMRI data and the microarray data were collected from different individuals. This is of course unavoidable when examining gene expression data, however, it is important to point out this limitation. One potential avenue for analysis would be to overlap connectivity patterns observed in fMRI with PET radioligand data of GABAa receptors. PET studies of GABAa receptor distribution has been extensively explored in schizophrenia.[44] This approach would allow for comparison between the effects of propofol on brain connectivity as measured by fMRI with overall GABAa receptor expression, however, it would not be possible to address potential differences in expression of GABAa receptor subtypes unless selective radioligands are generated. An additional limitation is that the participants in this study were not fully anaesthetised, but only moderately sedated. This means that our results may reflect an intermediate state between wakefulness and anaesthesia. Another limitation results from correlating the BOLD signal from fMRI to establish functional brain networks. Although brain connectivity as measured by fMRI is a well-established technique, it is limited in being a measure of blood oxygen concentration and not a direct measure of neuronal activity. Furthermore, it has a low sampling frequency, making it impossible to measure higher frequency brain network oscillations. Future work in this area should, in addition to fMRI, use electrophysiological methods to measure brain network oscillations.

Conclusions

Using functional connectivity and whole-brain human microarray data, we examined gene expression in brain regions that change their connectivity during propofol administration. Brain regions that are significantly altered by propofol sedation have high PV-expressing GABAergic interneurones. These results suggest that PV is particularly important for driving the change in brain connectivity and ultimately the loss of consciousness associated with propofol administration.

Authors' contributions

Conceived of and designed the experiment: RMA, EAS, MMC, BM, DKM
Performed the experiments: RMA, EAS
Analysed the data: MMC, BM, IP, EAS
Wrote and edited the manuscript: all authors
Study design: MMC, RMA, DKM, EAS
Study registration: RMA, DKM, EAS
Data interpretation: MMC, IP, BM, DKM, EAS
Statistical analysis: MMC, IP, BM, EAS
Primary manuscript preparation: MMC, EAS

Acknowledgements

The authors thank the radiographers at the Wolfson Brain Imaging Centre for their assistance in data acquisition.

Declarations of interest

The authors declare that they have no conflict of interest.

Funding

Grant from the Wellcome Trust: Clinical Research Training Fellowship to RA (grant number: 083660/Z/07/Z); National Institute for Health Research (NIHR, UK), Cambridge Biomedical Research Centre and NIHR Senior Investigator Awards to DKM; Canadian Institute for Advanced Research (CIFAR) to DKM and EAS (RCZB/072 RG93193); Stephen Erskine Fellowship (Queens' College, Cambridge) to EAS; British Oxygen Professorship of the Royal College of Anaesthetists to DKM. MC was supported by the Cambridge International Trust and the Howard Sidney Sussex Research Studentship. IP was supported by Downing College, University of Cambridge through a Treherne Studentship; This work was also supported by the NIHR Brain Injury Healthcare Technology Co-operative based at Cambridge University Hospitals NHS Foundation Trust and the University of Cambridge.

References

1. Rudolph U, Antkowiak B. Molecular and neuronal substrates for general anaesthetics. *Nat Rev Neurosci* 2004; **5**: 709–20
2. Jurd R, Arras M, Lambert S, et al. General anesthetic actions in vivo strongly attenuated by a point mutation in the GABAA receptor β3 subunit. *FASEB J* 2002; **2**: 250–2
3. Brown EN, Purdon PL, Van Dort CJ. General anesthesia and altered states of arousal: a systems neuroscience analysis. *Ann Rev Neurosci* 2011; **34**: 601–28
4. Yip GMS, Chen ZW, Edge CJ, et al. A propofol binding site on mammalian GABAA receptors identified by photolabeling. *Nat Chem Biol* 2013; **9**: 715–20
5. Fox MD, Raichle ME. Spontaneous fluctuations in brain activity observed with functional magnetic resonance imaging. *Nat Rev Neurosci* 2007; **8**: 700–11

6. Andrews-Hanna JR, Reidler JS, Sepulcre J, Poulin R, Buckner RL. Functional-anatomic fractionation of the brain's default network. *Neuron* 2010; **65**: 550–62
7. Boveroux P, Vanhaudenhuyse A, Phillips C. Breakdown of within-and between-network resting state during propofol-induced loss of consciousness. *Anesthesiology* 2010; **113**: 1038–53
8. Fox MD, Snyder AZ, Vincent JL, Corbetta M, Van Essen DC, Raichle ME. The human brain is intrinsically organized into dynamic, anticorrelated functional networks. *Proc Natl Acad Sci USA* 2005; **102**: 9673–9
9. Stamatakis EA, Adapa RM, Absalom AR, Menon DK. Changes in resting neural connectivity during propofol sedation. *PloS One* 2010; **5**: e14224
10. Tremblay R, Lee S, Rudy B. Review GABAergic interneurons in the neocortex: from cellular properties to circuits. *Neuron* 2016; **91**: 260–92
11. Hawrylycz MJ, Lein ES, Guillozet-Bongaarts AL, et al. An anatomically comprehensive atlas of the adult human brain transcriptome. *Nature* 2012; **489**: 391–9
12. Preller KH, Burt JB, Ji JL, et al. Changes in global and thalamic brain connectivity in LSD-induced altered states of consciousness are attributable to the 5-HT2A receptor. *eLIFE* 2018; **7**, e35082
13. Burt JB, Demirtaş M, Eckner WJ, et al. Hierarchy of transcriptomic specialization across human cortex captured by structural neuroimaging topography. *Nat Neurosci* 2018; **21**: 1251–9
14. Whitaker KJ, Vértes PE, Romero-Garcia R, et al. Adolescence is associated with genomically patterned consolidation of the hubs of the human brain connectome. *Proc Natl Acad Sci U S A* 2016; **113**: 9105–10
15. Chen CH, Panizzon MS, Eyler LT, et al. Genetic influences on cortical regionalization in the human brain. *Neuron* 2011; **72**: 537–44
16. Absalom AR, Mani V, De Smet T, Struys MM. Pharmacokinetic models for propofol-defining and illuminating the devil in the detail. *Br J Anaesth* 2009; **103**: 26–37
17. Marsh B, White M, Morton N, Kenny GN. Pharmacokinetic model driven infusion of propofol in children. *Br J Anaesth* 1991; **67**: 41–8
18. Ashburner J, Friston KJ. Unified segmentation. *Neuroimage* 2005; **26**: 83951
19. Craig MM, Manktelow AE, Sahakian BJ, Menon DK, Stamatakis EA. Spectral diversity in default mode network connectivity reflects behavioral state. *J Cogn Neurosci* 2018; **30**: 526–39
20. Whitfield-Gabrieli S, Nieto-Castanon A. Conn: a functional connectivity toolbox for correlated and anticorrelated brain networks. *Brain Connect* 2012; **2**: 125–41
21. Hagmann P, Cammoun L, Gigandet X, et al. Mapping the structural core of human cerebral cortex. *PLoS Biol* 2008; **6**: e159
22. Krishnan A, Williams LJ, Randal A, Abdi H. Partial Least Squares (PLS) methods for neuroimaging: a tutorial and review. *Neuroimage* 2011; **56**: 455–75
23. McIntosh AR, Misic B. Multivariate statistical analyses for neuroimaging data. *Annu Rev Psychol* 2013; **64**: 449–525
24. Misic B, Betzel RF, de Reus MA, et al. Network-level structure-function relationships in human neocortex. *Cereb Cortex* 2016; **26**: 3285–96
25. Efron B, Tibshirani R. Bootstrap methods for standard errors, confidence intervals, and other measures of statistical accuracy. *Stat Sci* 1986; **1**: 54–75
26. Smith SM, Fox PT, Miller KL, et al. Correspondence of the brain's functional architecture during activation and rest. *Proc Natl Acad Sci U S A* 2009; **106**: 13040–5
27. Traub RD, Whittington MA. Simulation of gamma rhythms in networks of interneurons and pyramidal cells. *J Comput Neurosci* 1997; **4**: 141–50
28. Fisahn A, Pike FG, Buhl EH, Paulsen O. Cholinergic induction of network oscillations at 40 Hz in the hippocampus. *Nature* 1998; **394**: 3–6
29. Sohal VS, Zhang F, Yizhar O, Deisseroth K. Parvalbumin neurons and gamma rhythms enhance cortical circuit performance. *Nature* 2009; **459**: 698–702
30. Huang Y, Yoon K, Ko H, et al. 5-HT3a receptors modulate hippocampal gamma oscillations by regulating synchrony of parvalbumin-positive interneurons. *Cereb Cortex* 2016; **26**: 576–85
31. Rudy B, Fishell G, Lee S, Hjerling-Leffler J. Three groups of interneurons account for nearly 100% of neocortical GABAergic neurons. *Dev Neurobiol* 2013; **71**: 45–61
32. Alkire MT, Hudetz AG, Tononi G. Consciousness and anesthesia. *Science* 2008; **322**: 876–80
33. John ER, Prichep LS, Kox W, et al. Invariant reversible QEEG effects of anesthetics. *Concious Cogn* 2001; **10**: 165–83
34. Phelps EA. Emotion and cognition: insights from studies of the human amygdala. *Annu Rev Psychol* 2006; **57**: 27–53
35. Meletis K, Carlén M, Meletis K, et al. Driving fast-spiking cells induces gamma rhythm and controls sensory responses. *Nature* 2009; **459**: 663–8
36. Carr MF, Karlsson MP, Frank LM. Transient slow gamma synchrony underlies hippocampal memory replay. *Neuron* 2012; **75**: 700–13
37. Buzsaki G, Leung LW, Vanderwolf CH. Cellular bases of hippocampal EGG in behaving rat. *Brain Res* 1983; **287**: 139–71
38. Buzsaki G, Wang X. Mechanisms of gamma oscillations. *Annu Rev Neurosci* 2012; **35**: 203–25
39. Barttfeld P, Bekinschtein TA, Salles A, et al. Factoring the brain signatures of anesthesia concentration and level of arousal across individuals. *Neuroimage Clin* 2015; **9**: 385–91
40. Di Perri C, Bahri MA, Amico E, et al. Neural correlates of consciousness in patients who have emerged from a minimally conscious state: a cross-sectional multimodal imaging study. *Lancet Neurol* 2016; **15**: 830–42
41. Vlisides PE, Li D, Zierau M, et al. Dynamic cortical connectivity during general anesthesia in surgical patients. *Anesthesiology* 2019; **130**: 885–97
42. Li D, Vlisides PE, Kelz MB, et al. Dynamic cortical connectivity during general anesthesia in healthy volunteers. *Anesthesiology* 2019; **130**: 870–84
43. Leech R, Kamourieh S, Beckman CF, et al. Fractionating the default mode network: distinct contributions of the ventral and dorsal posterior cingulate cortex to cognitive control. *J Neurosci* 2011; **31**: 3217–24
44. Egerton A, Modinos G, Ferrera D, McGuire P. Neuroimaging studies of GABA in schizophrenia: a systematic review with meta-analysis. *Transl Psychiatry* 2017; **7**: e1147

Handling editor: Hugh C Hemmings Jr